

Published in final edited form as:

Metallomics. 2016 October 01; 8(10): 1081–1089. doi:10.1039/c6mt00150e.

Metal-catalyzed oxidation of A β and the resulting reorganization of Cu binding sites promote ROS production†

Clémence Cheignon^{*,a,b,c}, Peter Fallert^{‡,a,b}, Denis Testemale^{d,e}, Christelle Hureau^{a,b}, and Fabrice Collin^{*,a,b,c}

^aLCC (Laboratoire de Chimie de Coordination), CNRS UPR 8241, 205 route de Narbonne, 31062 Toulouse Cedex 09, France

^bUniversité de Toulouse, UPS, INPT, 31077 Toulouse, France

^cUMR 152 Pharma Dev, Université de Toulouse, IRD, UPS, France

^dUniversity of Grenoble Alpes, Institut NEEL, F-38000 Grenoble, France

^eCNRS, Institut NEEL, F-38000 Grenoble, France

Abstract

In the context of Alzheimer's disease (AD), the production of HO \cdot by copper–amyloid beta (A β) in the presence of ascorbate is known to be deleterious for the A β peptide itself and also for the surrounding molecules, thus establishing a direct link between AD and oxidative stress. The metal-catalyzed oxidation (MCO) of A β primarily targets the residues involved in copper coordination during HO \cdot production. In the present work, we demonstrate that the oxidative damage undergone by A β during MCO lead to a change in copper coordination, with enhanced catalytic properties that increases the rates of ascorbate consumption and HO \cdot production, and the amount of HO \cdot released by the system. This phenomenon is observed after the peptide has been sufficiently oxidized.

Introduction

In 2012, 36 million people suffered from Alzheimer's disease (AD), the widespread neurodegenerative disease. A hallmark of this disease is the presence of senile plaques in the brain,¹ mainly composed of the amyloid- β peptide (A β)² in an aggregated form. The peptide is also found in a soluble form in healthy brains.³ A high concentration of metals, such as copper, zinc and iron, are also found in the plaques.^{4–6} Cu and Zn are bound directly to the A β peptide. Among them, copper is redox-active and can catalyze the production of Reactive Oxygen Species (ROS) when bound to A β .^{7–9} In the presence of dioxygen and a reductant such as ascorbate, the Cu–A β system can produce the superoxide anion (O $_2^{\cdot-}$), hydrogen peroxide (H $_2$ O $_2$) and the hydroxyl radical (HO \cdot) *in vitro*.^{8,10,11} The latter is the most reactive and can cause oxidative damage to the surrounding biomolecules,

This article is licensed under a [Creative Commons Attribution-NonCommercial 3.0 Unported Licence](#).

clemence.cheignon@lcc-toulouse.fr, fabrice.collin@univ-tlse3.fr; Tel: +33 (0)5 61 33 31 56.

[‡]Current address: Institut de Chimie (UMR 7177), 4 rue B. Pascal, F-67000 Strasbourg, France.

such as lipids, nucleic acids and proteins (with the rate constant usually ranging from 10^9 to 10^{10} L mol⁻¹ s⁻¹), including A β itself, which is found to be oxidized in amyloid plaques *in vivo*.¹³ The link between AD and oxidative stress is also supported by DNA oxidation, proteins and lipid peroxidation, as evidenced in the brain of AD patients.^{14,15}

The coordination mode of copper with A β is of interest for a better understanding of the metal-catalyzed ROS production. At physiological pH, two coordination modes with a square-planar geometry were identified for the Cu(II)-A β complex, called components I and II (Fig. 1a),^{16,17} involving in particular Asp1 and the His residues His6, 13 and 14. The two forms are in pH-dependent equilibrium with a pK_a value of 7.8.¹⁸ In addition, dynamic exchange between ligands on a given binding position is also observed.¹⁹ Cu(I) is linked to A β in a linear fashion by two of the three His residues present in the A β sequence, in a fast dynamic exchange between ligands.^{19,20} The major form involves His13 and His14 (Fig. 1b).

To catalyze the ROS production, copper has to cycle between its two redox states. As the coordination of Cu(I) and Cu(II) with A β is very different, the direct electron transfer between those two states (called the resting states) is too slow, due to the high requirement of rearrangement energy. The electron transfer rather proceeds *via* a low-populated redox-competent state, called the “in-between” state, for which Cu(I) and Cu(II) coordination with A β is close enough to allow minimal energy for reorganization.^{21,22}

The metal-catalyzed oxidation (MCO) of A β by the Cu-A β /ascorbate/O₂ system has been previously studied.^{21,23,24} Because ROS are produced at the metal center, the A β peptide residues are the preferential targets for an HO[•] attack. In line with their involvement in copper coordination in the “in-between” state of Cu-A β ,²¹ Asp1, His13 and His14 are the major oxidized residues (Fig. 2). Asp1 oxidation was proposed to lead to the formation of either an isocyanate or a pyruvate function *via* oxidative cleavage or decarboxylation and deamination, respectively,^{21,25} while His13 and 14 are found to be oxidized into 2-oxohistidines.^{21,23,24} The oxidation of Asp1 was found to be three times higher than the oxidation of histidine, with decarboxylation/deamination as a preferential mechanism (5 times higher than the oxidative cleavage).

Thus, the oxidation of the major ligands leading to the oxidized A β peptide (A β ox as named below), could have an impact on the coordination sites of copper with A β . The impact could be different for the two oxidation degrees of both the resting and “in-between” states of Cu-A β . These structural changes might result in a modification of the catalytic properties of the complex.

Thus, in the present study, we report first on the consequence of the oxidation of the A β peptide on the coordination of Cu(I) and Cu(II) resting states by X-ray absorption near edge spectroscopy (XANES) and electron paramagnetic resonance (EPR). Then we analyze the impact of A β oxidation on the Cu-induced ROS production by mass spectrometry, UV-visible and fluorescence spectroscopies.

Experimental

Chemicals

The Cu(II) used was from CuSO₄·5(H₂O) and purchased from Sigma. A stock solution of Cu(II) (10 mM) was prepared in ultrapure water. Phosphate buffer was bought from Sigma-Aldrich and dissolved in ultrapure water to reach a 100 mM concentration and pH 7.4. HEPES buffer was bought from Sigma and dissolved in ultrapure water to reach a 0.5 M concentration and pH 7.1. Ascorbate solutions were freshly prepared a few minutes prior to each experiment by dissolving sodium L-ascorbate (Sigma) in ultrapure water. Hydrogen peroxide (H₂O₂) solutions were freshly prepared from a 30 wt% H₂O solution purchased from Sigma-Aldrich. A stock solution of coumarin-3-carboxylic acid (CCA) 1 mM (from Sigma) was prepared in phosphate buffer (0.1 M, pH 7.4) at room temperature. Ethylene diamine tetraacetic acid (EDTA) was purchased from Sigma-Aldrich and dissolved in ultrapure water to reach a concentration of 40 mM. Sodium dithionite was bought from Sigma-Aldrich and dissolved in ultrapure water a few minutes prior to each experiment.

Peptides

All the synthetic peptides were bought from GeneCust (Dudelange, Luxembourg), with a purity grade of >95%. Stock solutions of A β ₂₈ (sequence DAEFRHDSGYEVHHQKLVFFAEDVGSNK), AcA β ₂₈ (sequence Ac-DAEFRHDSGYEVHHQKLVFFAEDVGSNK), A β ₇ (sequence DAEFRHD), A β ₁₆ (sequence DAEFRHDSGYEVHHQK), AcA β ₁₆ (Ac-DAEFRHDSGYEVHHQK) and D7H-A β ₁₆ (sequence DAEFRHDSGYEVHHQK) peptides were prepared by dissolving the powder in ultrapure water (resulting pH \approx 2). The peptide concentration was then determined by UV-visible absorption of Tyr10 considered as free tyrosine (at pH 2, ($\epsilon_{276} - \epsilon_{296}$) = 1410 M⁻¹ cm⁻¹). For A β ₇, the absorption of Phe (($\epsilon_{258} - \epsilon_{280}$) = 190 M⁻¹ cm⁻¹) was used.

Oxidation of the A β peptide

The A β ₂₈ peptide (60 μ M) was oxidized in a phosphate buffered solution (50 mM, pH 7.4) containing Cu(II) (50 μ M) and ascorbate (0.5 mM) for 30 min. Then, the solution was concentrated with a Amicon Ultra 3 kDa membrane (Millipore), washed with EDTA (10 equiv.) to remove copper, then with water and finally with NaOH (50 mM, pH \approx 13). The oxidized peptide solution was recovered and the concentration of the oxidized A β peptide was then determined through the UV-visible absorption of Tyr10, considered as free tyrosine (($\epsilon_{293} - \epsilon_{360}$) = 2400 M⁻¹ cm⁻¹) in NaOH (50 mM, resulting pH \approx 13).

As the oxidized peptide solution has a background absorbance at 293 nm, the curve is fitted to subtract the absorbance due to the tailing (see Fig. S1, ESI[†]) from the Tyr absorption. The A β ₂₈ peptide was used for technical reasons (membrane cut-off of 3 kDa).

HO[•] production monitoring

Fluorescence experiments were performed on a multi-plate reader FLUOstar Optima 96-well plate reader system (BMG Labtech) at 25 °C. Two automatic injectors were used to add ascorbate and hydrogen peroxide solutions into the wells during experiments. Coumarin-3-

carboxylic acid (CCA) was used as a probe to detect HO[•], as it reacts with CCA to form 7-hydroxycoumarin-3-carboxylic acid (7-OH-CCA), which is fluorescent at 452 nm upon excitation at 395 nm. The intensity of the fluorescence signal is proportional to the number of 7-OH-CCA molecules formed, which in turn is proportional to the HO[•] radicals released. 26 A fixed volume of 2 μL of ascorbate (2 mM) and 2 μL of hydrogen peroxide (5 mM) were added every 15 min for 2 hours to 200 μL of phosphate buffered (pH 7.4, 50 mM) solutions containing CCA (0.5 mM) and Cu(II) (20 μM) with or without the Aβ peptide (Aβ₁₆, Aβ₇, AcAβ₁₆, D7H-Aβ₁₆, Aβ₂₈, AcAβ₂₈, or Aβ₄₀) (25 μM). The fluorescence was monitored every 30 s.

Ascorbate consumption experiments

UV-Vis spectra were recorded on an Agilent 8453 UV-visible spectrophotometer at 25 °C. The intensity of the ascorbate (Asc) absorption band at $\lambda = 265$ nm ($\epsilon = 14\,500$ M⁻¹ cm⁻¹) was monitored as a function of time, in 50 mM phosphate buffer, pH 7.4 containing 10 μM of Cu(II), 12 μM of peptide and 100 μM of Asc.

EPR measurements

EPR spectra were recorded on a Bruker Elexsys E500 spectrometer equipped with a continuous flow cryostat (Oxford). Analysis was performed using an aqueous solution containing 10% of glycerol, ⁶⁵Cu (450 μM) and peptide (500 μM). The pH was adjusted to 12.5 with NaOH (1 M). Experimental parameters were set as follows: $T = 120$ K, $\nu = 9.5$ GHz, microwave power = 20.5 mW, amplitude modulation = 10.0 G, and modulation frequency = 100 kHz.

Mass spectrometry

High Performance Liquid Chromatography/High Resolution Mass Spectrometry (HPLC/HRMS) analysis was performed on a LTQ-Orbitrap XL mass spectrometer (Thermo Fisher Scientific, Les Ulis, France), equipped with an electrospray ionization source, and coupled to an Ultimate 3000 LC System (Dionex, Voisins-le-Bretonneux, France). The sample (10 μL) was injected onto the column (Phenomenex, Synergi Fusion RP-C18, 250 × 1 mm, 4 μm) at room temperature. Gradient elution was carried out with formic acid 0.1% (mobile phase A) and acetonitrile/water (80/20 v/v) formic acid 0.1% (mobile phase B) at a flow-rate of 50 μL min⁻¹. The mobile phase gradient was programmed with the following time course: 12% mobile phase B at 0 min, held for 3 minutes, linear increase to 100% B at 15 min, held for 4 min, and linear decrease to 12% B at 20 min and held for 5 min. The mass spectrometer was used as a detector, working in the full scan positive mode between 50 and 2000 Da. The Orbitrap cell was operated in the full-scan mode at a resolution power of 60 000. HPLC/HRMS was also used to check for digestion efficiency, systematically found close to 100% (non-digested peptides were not detected).

Proteolytic digestion

The solution of Aβ was filtered using an Amicon 3 kDa centrifugal device (Millipore) by centrifugation for 15 min at 13 500 rpm, then washed and centrifuged twice with 200 μL sodium hydrogenocarbonate (100 mM, pH 8). The concentrated sample (approx. 50 μL) was

recovered and transferred to an Eppendorf ProteinLoBind 1.5 mL vial. Trypsin (0.05 ng μL^{-1} in formic acid 0.1%) was added to obtain an A β /trypsin ratio of 20/1 (w/w) and digestion was carried out at 37 °C for 3 h in a Thermomixer (Eppendorf), with 10 s mixing at 750 rpm every min.

Cu K-edge X-ray absorption measurements

The copper-containing A β (A β_{28} , A $\beta_{28\text{ox}}$ or A β_7) solutions were injected into sample holders in between two Kapton windows (3 M, cat. #1205; Minneapolis, MN) and immediately frozen in liquid nitrogen. All samples were maintained at 10–20 K throughout data collection using a helium cryostat. Cu K-edge XANES (X-ray absorption near edge structure) spectra were recorded at the BM30B (FAME) French CRG beamline at the European Synchrotron Radiation Facility (ESRF, Grenoble, France).²⁷ The storage ring was operated in a uniform mode at 6 GeV with a 200 mA current. The beam energy was selected using an Si(220) N₂ cryocooled double-crystal monochromator with an experimental resolution of ~0.5 eV.²⁸ The beam spot on the sample was approximately 200 × 100 μm^2 ($H \times V$, FWHM). The spectra were collected in a fluorescence mode using a 30-element Ge solid-state fluorescence detector (Canberra). The energy was calibrated with Cu metallic foils, such that the maximum energy of the first derivative was set at 8979 eV. Cu data were collected from 8830 to 8960 eV using 5 eV step and 2 s counting time, from 8960 to 9020 eV using 0.5 eV step and 3 s counting time, and from 9020 to 9300 eV with a k -step of 0.05 \AA^{-1} and the counting time increasing from 2 to 10 s.

For each sample, three spectra were averaged and the resulting XANES spectra were background-corrected by linear regression through the pre-edge region and a polynomial through the post-edge region and normalized to the edge jump. The beam was moved to a different position on the sample for each scan to avoid potential Cu photoreduction. All spectra were individually inspected prior to data averaging to ensure that beam damage was not occurring.

Cu(I) samples were prepared under a continuous flow of N₂ by direct addition (10 equiv.) of fresh made sodium dithionite (Na₂S₂O₄) stock solution (0.1 M) into the sample holder containing CuSO₄ (0.9 mM) and the peptide (1 mM) in the presence of 10% glycerol as a cryoprotectant with the pH adjusted to 7.1. The sample was immediately frozen in liquid nitrogen. Under such conditions, no significant pH drift due to the addition of Na₂S₂O₄ was measured.

Results

Introductory remarks

This study focused on two peptides, A β_{16} and A β_{28} , as valuable counterparts of the full-length peptides. These two short peptides are: (i) valuable models for studying copper coordination and ROS production since copper binds to the N-terminal part of A β (16 first residues)^{29–32} and (ii) easier to handle than the full-length peptide (A $\beta_{40/42}$), which is more prone to aggregation.

In the first three parts of the paper, where oxidized A β (A β ox) is under focus, the A β ₂₈ peptide was used as well as the truncated A β ₇ peptide and the acetylated A β ₂₈ peptide (AcA β ₂₈). A β ₇ only bears one histidine residue, and is thus a valuable model to mimic His13 and His14 oxidation reactions. AcA β ₂₈ has a blocked N-terminal moiety and is an appropriate model to mimic Asp1 oxidation, as its N-terminal amine is not involved anymore in Cu(II) coordination.

In the last part describing the evolution of HO \cdot release during A β oxidation, the A β ₁₆ peptide is used for comparison with the truncated A β ₇ peptide, the acetylated A β ₁₆ (AcA β ₁₆) and the mutated D7H–A β ₁₆. The latter is a familial AD mutation resulting in a peptide with 1 His more than A β ₁₆, thus its study is both of mechanistic and biological interest.

A β ox refers to a mixture of biologically oxidized species (see Fig. S2, ESI $^+$). Complete elucidation of the nature as well as the proportion of various oxidized species might be of interest. However, for the present study, knowing the main oxidation reactions that have been previously reported²¹ is sufficient.

Coordination of copper to A β ox

As previously shown,^{21,23,24} the HO \cdot radicals produced by the Cu/A β /ascorbate/O₂ system are deleterious for the A β peptide itself. Because they are generated at the metal center, several residues of A β involved in Cu(I) and Cu(II) coordination (namely Asp1, His13 and His14) are oxidized, leading to A β ox. The oxidation of A β leads to the formation of a mixture of peptides with different oxidation sites. The experimental conditions for peptide oxidation have been previously studied.³³ In the present study, the A β ₂₈ peptide was oxidized in the presence of 0.8 equiv. of copper and 8 equiv. of ascorbate, in order to ensure that 80% of the peptide is oxidized (at least one amino acid residue is oxidized) (Fig. S3, ESI $^+$). At the end of the reaction, the oxidized peptide (A β ox) was purified using membrane filtration to completely remove any remaining copper bound to the peptide (see the Experimental section), then quantified by UV-Vis and Cu was added again to A β ox or A β ₂₈ for the spectroscopic studies of Cu(I) and Cu(II) coordination.

Cu(I) coordination to A β ox—X-ray absorption near edge spectroscopy (XANES) is a very sensitive tool to probe the Cu(I) environment. It has been successfully applied to the spectroscopy of silent metal ions bound to flexible peptides. The XANES spectra of the three Cu(I) samples were collected: Cu(I) coordinated to the non-oxidized A β peptide, to the oxidized A β peptide (A β ox) and to the truncated A β ₇ peptide (Fig. 3). A β ₇, bearing only the His at position 6, was chosen as a model for Cu(I)-binding to the oxidized peptide since His13 and His14 are the primary targets of oxidation and thus supposed to lose their efficiency in Cu coordination. Single His mutants were not studied since it is anticipated that the oxidation of one of the three His does not affect the coordination much. Indeed, Cu(I) coordination requires only two His residues, as proved by NMR studies^{20,34} or by affinities of single His–Ala mutation of the A β peptide.^{34–36} In Fig. 3, the pre-edge feature at 8982 eV, assigned to the 1s \rightarrow 4p electric dipole allowed transition, is visible. Its intensity is characteristic of a Cu(I) species coordinated to 2 ligands in a linear fashion in A β –Cu(I),³⁷

as previously reported.^{20,32,38,39} The intensity is lower for $A\beta_7$, indicating an increment of the number of ligands,³⁷ likely one His of the peptide and 2 or 3 ligands from the solvent. In the case of the $Cu(I)-A\beta_{ox}$ species, this pre-edge signature tends to be closer to that obtained for $Cu(I)-A\beta_7$. At a higher energy, in particular around 8985, 8995, 9050 and 9075 eV (arrows in the inset of Fig. 3), the XANES spectrum of $A\beta_{28ox}$ shows features that are intermediate between the ones of $Cu(I)-A\beta_{28}$ and the ones of $Cu(I)-A\beta_7$ (Fig. 3). A linear combination fitting of the XANES provides the relative contribution of the two possible coordination modes: 40% of $Cu(I)$ is coordinated as in $Cu(I)-A\beta_7$ (Fig. S4, ESI[†]), and the other part of $Cu(I)$ is coordinated to the peptide as in $Cu(I)-A\beta$, with 2 His. This is consistent with the oxidative damage undergone by both His13 and His14 residues during $A\beta$ oxidation²¹ that would disrupt the normal coordination of copper in $A\beta-Cu(I)$, known to involve the same residues.²⁰

$Cu(II)$ coordination to $A\beta_{ox}$ —The potential change in the coordination of $Cu(II)$ to $A\beta_{ox}$ was studied by Electron Paramagnetic Resonance (EPR). The comparison of the signature of $Cu(II)-A\beta_{ox}$ and $Cu(II)-A\beta_{28}$ at pH 7.4 shows a coordination change of a part of the Cu , however interpretation is not conclusive (Fig. S5, ESI[†]). Hence to probe the $Cu(II)$ environment inside $A\beta_{ox}$ and the integrity of the N-terminal amine, we also performed EPR studies at a higher pH. At pH 12.5, the EPR spectrum of $Cu(II)-A\beta_{ox}$ is indeed different to the one of $Cu(II)-A\beta_{28}$ and somehow reminiscent to the one of $Cu(II)-AcA\beta_{28}$ ^{35,36,40} (Fig. 4), where $AcA\beta_{28}$ is the N-terminal acetylated counterpart of $A\beta_{28}$. The fingerprint is actually an intermediate between those of $Cu(II)-A\beta_{28}$ and $Cu(II)-AcA\beta_{28}$. It was fitted through a linear combination (Fig. S6, ESI[†]) with 40% of $Cu(II)-AcA\beta_{28}$ and 60% of $Cu(II)-A\beta_{28}$. This shows that for 40% of the $A\beta_{ox}$ species in solution, the terminal $-NH_2$ is no longer involved in $Cu(II)$ coordination in line with the Asp1 oxidative damage of the peptide previously described.^{21,24,25} Probing the impact of His oxidation by EPR is hazardous since at pH 7.4 only a modification in the repartition between components I and II are expected, while at pH 12.5 the His residues are not involved anymore in $Cu(II)-A\beta_{28}$.³⁰

In brief, our data are in line with the interpretation that $Cu(II)-A\beta_{ox}$ complexes include a significant proportion of binding sites similar to those of $Cu(II)-AcA\beta_{28}$ due to Asp1 oxidation, while His oxidation reactions induce the formation of $Cu(I)-A\beta_7$ like species.

HO[•] production by $Cu-A\beta_{ox}$

The metal-catalyzed oxidation of $A\beta$ leads to a change in both $Cu(II)$ and $Cu(I)$ coordination sites that would impact $Cu(I)$ and $Cu(II)$ affinities both in the resting and “in-between” states. Regarding $Cu(I)$ binding, it has been previously shown that a single His–Ala mutation does not change the affinity significantly^{34–36} while a double His–Ala mutation induces a decrease of about two orders of magnitude.³⁵ For $Cu(II)$, the prevention of N-terminal amine binding also leads to a decrease of about two orders of magnitude^{35,40,41} while two His–Ala mutations have only a slight impact.³⁵ Hence the oxidation of the $A\beta$ peptide induces a general decrease in the $Cu(I)$ or $Cu(II)$ affinity although it is not possible to quantify it for the “in-between” state. As a consequence, the oxidation of the $A\beta$ peptide and the resulting modification of the Cu sites could (i) increase the rate of ROS production as a direct impact

and (ii) result in a contribution of free Cu in the global ROS production as an indirect effect due to the decrease of Cu affinity for A β ox.

In the present work, the production of HO \cdot was studied by both ascorbate oxidation, monitored by UV-visible spectroscopy, and the fluorescence of 7-OH-CCA, an oxidation product of CCA resulting from HO \cdot scavenging. The 7-OH-CCA fluorescence is proportional to the HO \cdot quantity trapped by CCA.³³ The production of HO \cdot was compared between Cu-A β ₂₈, Cu-A β ox and Cu-A β ₇ (Fig. 5).

The rate of both ascorbate oxidation and 7-OH-CCA formation is much higher for free copper than for Cu-A β , in line with the literature.^{8,42–45} Then, the rate of ascorbate consumption has the following order: A β ₇ > A β ox > A β ₂₈ (Fig. 5a). A similar trend is obtained for the rate (gradient of the curve) of HO \cdot production (Fig. 5b). In particular, Cu bound to the oxidized peptide reacts to consume ascorbate and produce HO \cdot faster than Cu linked to the non-oxidized peptide. The catalytic behavior of copper bound to A β ox is between Cu-A β ₂₈ and Cu-A β ₇, in line with the binding mode of Cu(I) to A β ox which includes peptide with two oxidation reactions on the His residues and with the lower affinity of A β ox for copper. Thus, the binding mode of copper to A β is affected by A β oxidation, which in turn increases its catalytic activity for the production of ROS. As shown above by XANES and EPR experiments, the coordination of copper in the resting states is modified upon A β oxidation. The higher catalytic activity of Cu-A β ox and the resulting faster HO \cdot production show that the coordination of Cu(I) and Cu(II) within the “in-between” state (the only redox-competent species) is also modified.

The quantity of ROS released by the Cu-peptide system (corresponding to the HO \cdot available for the oxidative damage of exogenous molecules) has also been evaluated. It is given by the fluorescence value at the plateau. The total amount of HO \cdot trapped by CCA follows the trend: A β ₇ \gg A β ox > A β ₂₈ (Fig. 5b, plateau of the curve), in line with a partial decrease of the A β ox ability to trap HO \cdot .

Effect of H₂O₂ on A β oxidation and ascorbate consumption

In the above studies, A β oxidation was induced by the ROS produced by the Cu-A β /ascorbate system, in the presence of molecular oxygen. The hydroxyl radical (HO \cdot) produced by the Fenton-like reaction catalyzed by copper (Scheme 1) is the most reactive one and thus supposed to be mainly responsible for the oxidation of the A β residues. The other two ROS produced by the system, hydrogen peroxide and the superoxide anion, may react in some cases with a specific target, for instance with methionine residues in peptides and proteins, to form methionine sulfoxide. However, they are much less reactive than the hydroxyl radical. We were interested in comparing the behavior of the system, in terms of A β oxidation and ascorbate consumption, in the presence or absence of hydrogen peroxide, in order to evaluate the catalytic properties of the system and identify the targeted residues under these experimental conditions. As hydroxyl radicals are the sole species produced in the presence of H₂O₂, such a comparison should also provide information on the reactivity of O₂ and O₂^{•-} with A β during MCO.

The MCO of A β was compared after 1, 2 or 3 successive additions of ascorbate or ascorbate and H₂O₂. The presence of H₂O₂ in solution leads to a 3 times higher oxidation of A β compared to the absence of H₂O₂ (Fig. 6a). This is in line with the expectation that A β oxidation is mainly due to HO \cdot , based on the known mechanism of ROS production by Cu–A β for which the production of HO \cdot is 3 times higher in the presence of H₂O₂ compared to the absence of H₂O₂ (Scheme 1). Indeed, in the absence of H₂O₂, 3 electrons (and hence 1.5 ascorbate) are needed to form one HO \cdot . In the presence of H₂O₂ only one electron is needed to produce one HO \cdot . There is no remaining non-oxidized A β peptide after 3 successive additions of ascorbate and H₂O₂, meaning that at least one amino acid residue of A β is oxidized. At the same time, the ascorbate consumption rate is also higher in the presence of hydrogen peroxide (Fig. 6b). The first electron transfer from Cu(I) to O₂ is the rate limiting step of ROS production by Cu–A β ; adding H₂O₂ eliminates this step and thus increases the ascorbate consumption rate.

The oxidative damage on A β has been characterized using HPLC/HRMS after MCO in the presence or absence of H₂O₂ (Fig. 7). As expected, the oxidative damage undergone by A β is the same in the presence or absence of H₂O₂. This tends to indicate that the hydroxyl radical is mainly responsible for them. Asp1, His13 and His14 are the three major targets of HO \cdot attack during metal-catalyzed oxidation. Their generation is dependent on the amount of ascorbate and H₂O₂ added in the solution: the higher the number of additions of ascorbate or ascorbate/H₂O₂, the higher the level of A β oxidation. Moreover, the presence of H₂O₂ exacerbates the effect (Fig. 7b) as the chromatographic peaks reach a higher level than in the absence of H₂O₂ (Fig. 7a) for a given [Asc]. This is in line with the higher degradation of A β in the presence of H₂O₂ (Fig. 7a). Thus, the presence of H₂O₂ (1) leads to the same oxidative damage of A β and (2) achieves a higher degradation state of A β per oxidized ascorbate. In other words, it is possible to achieve the same A β degradation state with 3 times less successive additions of ascorbate in the presence of H₂O₂, because the system is more efficient in producing HO \cdot radicals.

Evolution of HO \cdot release by Cu–A β upon oxidation

The above studies done with A β ox have been carried out after 80% of the peptide is oxidized. We also aim to understand how the oxidation of the peptide impacts the HO \cdot release for different oxidation states of the peptide. The native A β ₁₆ peptide as well as the truncated or mutated peptides A β ₇, AcA β ₁₆ and D7H–A β ₁₆ were studied and compared (see the Introductory remarks for more details on the peptides).

In order to study the HO \cdot release by Cu–A β at increasing degrees of peptide oxidation, successive fixed amounts of ascorbate and hydrogen peroxide were added to the solution containing the Cu–A β complex. Based on the observation that with or without H₂O₂ the same damage occurs (Fig. 7), we used the system with H₂O₂ due to practical reasons (to avoid excessive dilution and HO \cdot trapping at a very high ascorbate concentration³³). The fluorescence intensity was measured at the end of the reaction (at the plateau) and thus provided information on the total amount of HO \cdot trapped by CCA for each addition of ascorbate and H₂O₂ (fluorescence curves are given in the ESI,† Fig. S12).

Fig. 8 shows the fluorescence at the plateau as a function of the number of ascorbate and H_2O_2 additions for free Cu (Fig. 8a) and for Cu coordinated to the peptides (Fig. 8b–e). The highest fluorescence was obtained with free copper (Fig. 8a) because the maximum HO^\bullet radicals are trapped by CCA (no peptide in solution). A similar result is obtained when copper is coordinated to $\text{A}\beta_7$ (Fig. 8b), with a slightly lower gradient of the curve. This indicates that with $\text{A}\beta_7$, only a small quantity of HO^\bullet is trapped by the peptide and therefore only a small fraction of Cu is bound to $\text{A}\beta_7$ under these conditions (*i.e.* very diluted compared to spectroscopic studies). Copper, when coordinated to $\text{A}\beta_{16}$, $\text{AcA}\beta_{16}$ or $\text{D7H-A}\beta_{16}$, exhibits a strongly different behavior regarding the total amount of the HO^\bullet trapped by CCA (Fig. 8c–e). The total fluorescence after each addition of ascorbate and H_2O_2 is much lower than that of free copper, resulting in much lower gradients. As the HO^\bullet are produced at the metal center and because the peptide is coordinated to Cu, $\text{A}\beta$ is the first target for the radical attack. This results in a strong decrease in the HO^\bullet radicals directly trapped by CCA.

In addition, the curves exhibit two different linear parts, the first one with a low gradient is obtained for the 3–4 first additions of ascorbate and H_2O_2 , and the second one with a higher gradient is obtained after several additions of ascorbate and H_2O_2 . The modification of the N-terminal part of the peptide does not appear to affect the HO^\bullet release, as the gradients are similar for $\text{Cu-A}\beta_{16}$ and $\text{Cu-AcA}\beta_{16}$ (Fig. 8c and d). A comparable gradient is also obtained for $\text{Cu-(D7H-A}\beta_{16})$ (Fig. 8e), for the first part of the curve. A similar behavior is observed with the longer $\text{A}\beta_{28}$ and $\text{A}\beta_{40}$ peptides (ESI,† Fig. S13).

The higher gradients observed in the second part of the fluorescence curves (Fig. 8c–e) can be linked to a change in copper coordination due to peptide oxidation by HO^\bullet . The increase in the slopes is observed after 3 additions of ascorbate and H_2O_2 for $\text{A}\beta$ (Fig. 8c), *i.e.* after the peptide has been mostly oxidized at least once (Fig. 6a). The break of the curve for $\text{D7H-A}\beta_{16}$ (Fig. 8e) occurs after 4 additions of ascorbate and H_2O_2 instead of 3 additions for $\text{A}\beta_{16}$ (Fig. 8c). $\text{D7H-A}\beta_{16}$ has one more His residue than $\text{A}\beta_{16}$ and thus one additional target for HO^\bullet and one supplementary position for copper coordination. Supplementary addition of ascorbate and H_2O_2 is thus needed so that the peptide is sufficiently oxidized and the quantity of HO^\bullet scavenged by CCA increases.

This is in line with data shown in Fig. 9, where fluorescence was compared at different $\text{A}\beta/\text{Cu}$ ratios: 12/10 (blue curve) and 20/10 (grey curve). The break of the curve is no longer observed at the highest ratio 20/10, indicating that throughout the 8 successive additions of ascorbate and hydrogen peroxide, the total amount of HO^\bullet trapped by CCA remains constant. The $\text{A}\beta$ peptide is still oxidized and it would lose its efficiency in coordinating copper. However, the resulting loosely bound copper would be further coordinated by the part of the non-oxidized $\text{A}\beta$ peptide that remains in solution.

By comparison of the fluorescence gradients after 3 additions of ascorbate and hydrogen peroxide (Fig. 8c, first and second gradients), it appears that the $\text{A}\beta$ peptide is oxidized to the point of being two to three times less efficient in HO^\bullet scavenging but still two times more efficient than the $\text{A}\beta_7$ peptide (Fig. 8b). This is in line with a Cu center mainly bound to the $\text{A}\beta_{\text{ox}}$ peptide but not to the $\text{A}\beta_7$ peptide.

Concluding remarks

As shown above, the metal catalyzed oxidation of the A β peptide leads to a change in copper coordination for both the Cu(I) and Cu(II) resting states as probed, respectively, by XANES and EPR and it is anticipated that this is also true for the catalytic species involved in ROS production, the “in-between” state. Indeed, it was previously described that the production of HO \cdot radicals by the A β -copper system proceeds *via* an “in-between” state involving Asp1, His13 and His14 in the coordination sphere of copper.²¹ A similar oxidative protein and its consequences on the Cu binding site and on the enzyme activity have been recently reported for the Cu, Zn SOD, in the presence of H₂O₂⁴⁷ and in the presence of Cu/asc/O₂ as a model system.⁴⁸

Such coordination modifications impact the rate of HO \cdot production *via* two additive mechanisms: (i) a direct one due to a different binding site in the “in-between” state that has faster kinetics and (ii) an indirect one, relying on a decrease in Cu binding affinities for A β ox. This latter mechanism leads to a significant amount of free Cu under diluted conditions that would contribute to enhanced ROS production. In addition, the oxidation of the A β peptide induces a less efficient scavenging of the HO \cdot that could be due to a different Cu coordination site as discussed above or/and to a lower number of potential targets on the peptide. It was indeed previously shown that the oxidation of the A β residues stops after a certain reaction time, showing that HO \cdot is no longer trapped by A β .²¹

In a more biological environment, A β oxidation by the Cu–A β complex triggers a positive feedback loop that leads to a more deleterious oxidative stress due to both an enhanced ROS production rate and a decreased HO \cdot scavenging ability.

Supplementary Material

Refer to Web version on PubMed Central for supplementary material.

Acknowledgements

The authors acknowledge L. Debrauwer and E. Jamin for providing the Orbitrap mass spectrometer (MetaToul-AXIOM, INRA, UMR1331 Toxalim, Toulouse, France) and the ESRF for provision of synchrotron radiation on the FAME beamline (Proposal 30-02-1099). L. Rechinat is acknowledged for EPR experiments and M. Jones is acknowledged for the preparation of oxidized peptide and the UV-Vis spectra. This work was supported by the French National Agency of Research (ANR-13-BSV5-0016). C. H. thanks the ERC aLzINK – Contract no. 638712 for their financial support.

Notes and references

1. Selkoe DJ. *Science*. 2002; 298:789. [PubMed: 12399581]
2. Glenner GG, Wong CW. *Biochem Biophys Res Commun*. 1984; 120:885. [PubMed: 6375662]
3. Haass C, Schlossmacher MG, Hung AY, Vigo-Pelfrey C, Mellon A, Ostaszewski BL, Lieberburg I, Koo EH, Schenk D, Teplow DB, Selkoe DJ. *Nature*. 1992; 359:322. [PubMed: 1383826]
4. Lovell MA, Robertson JD, Teesdale WJ, Campbell JL, Markesbery WR. *J Neurol Sci*. 1998; 158:47. [PubMed: 9667777]
5. Miller LM, Wang Q, Telivala TP, Smith RJ, Lanzirotti A, Miklossy J. *J Struct Biol*. 2006; 155:30. [PubMed: 16325427]
6. Leskovjan AC, Lanzirotti A, Miller LM. *NeuroImage*. 2009; 47:1215. [PubMed: 19481608]

7. Huang X, Atwood CS, Hartshorn MA, Multhaup G, Goldstein LE, Scarpa RC, Cuajungco MP, Gray DN, Lim J, Moir RD. *Biochemistry*. 1999; 38:7609. [PubMed: 10386999]
8. Hureau C, Faller P. *Biochimie*. 2009; 91:1212. [PubMed: 19332103]
9. Opazo C, Huang X, Cherny RA, Moir RD, Roher AE, White AR, Cappai R, Masters CL, Tanzi RE, Inestrosa NC, Bush AI. *J Biol Chem*. 2002; 277:40302. [PubMed: 12192006]
10. Smith DG, Cappai R, Barnham KJ. *Biochim Biophys Acta, Biomembr*. 2007; 1768:1976.
11. Reybier K, Ayala S, Alies B, Rodrigues JV, Bustos Rodriguez S, La Penna G, Collin F, Gomes CM, Hureau C, Faller P. *Angew Chem, Int Ed*. 2016; 55:1085.
12. Farhataziz RA, Ross A. Hydroxyl radical and perhydroxyl radical and their radical ions, NSRDS-NBS. 1977; 59
13. Näslund J, Schierhorn A, Hellman U, Lannfelt L, Roses AD, Tjernberg LO, Silberring J, Gandy SE, Winblad B, Greengard P. *Proc Natl Acad Sci U S A*. 1994; 91:8378. [PubMed: 8078890]
14. Barnham KJ, Masters CL, Bush AI. *Nat Rev Drug Discovery*. 2004; 3:205. [PubMed: 15031734]
15. Sayre LM, Perry G, Smith MA. *Chem Res Toxicol*. 2008; 21:172. [PubMed: 18052107]
16. Hureau C. *Coord Chem Rev*. 2012; 256:2164.
17. Migliorini C, Porciatti E, Luczkowski M, Valensin D. *Coord Chem Rev*. 2012; 256:352.
18. Hureau C, Dorlet P. *Coord Chem Rev*. 2012; 256:2175.
19. Hureau C, Coppel Y, Dorlet P, Solari PL, Sayen S, Guillon E, Sabater L, Faller P. *Angew Chem, Int Ed*. 2009; 48:9522.
20. Hureau C, Balland V, Coppel Y, Solari PL, Fonda E, Faller P. *JBIC, J Biol Inorg Chem*. 2009; 14:995. [PubMed: 19618220]
21. Cassagnes L-E, Hervé V, Nepveu F, Hureau C, Faller P, Collin F. *Angew Chem, Int Ed*. 2013; 52:11110.
22. Balland V, Hureau C, Saveant J-M. *Proc Natl Acad Sci U S A*. 2010; 107:17113. [PubMed: 20858730]
23. Inoue K, Garner C, Ackermann BL, Oe T, Blair IA. *Rapid Commun Mass Spectrom*. 2006; 20:911. [PubMed: 16470704]
24. Kowalik-Jankowska T, Ruta M, Wi niewska K, Łankiewicz L, Dyba M. *J Inorg Biochem*. 2004; 98:940. [PubMed: 15149800]
25. Inoue K, Nakagawa A, Hino T, Oka H. *Anal Chem*. 2009; 81:1819. [PubMed: 19173589]
26. Manevich Y, Held KD, Biaglow JE. *Radiat Res*. 1997; 148:580. [PubMed: 9399704]
27. Proux O, Biquard X, Lahera E, Menthonnex JJ, Prat A, Ulrich O, Soldo Y, Trevisson P, Kapoujyan G, Perroux G, Taunier P, et al. *Phys Scr, T*. 2005; 115:970.
28. Proux O, Nassif V, Prat A, Ulrich O, Lahera E, Biquard X, Menthonnex JJ, Hazemann JL. *J Synchrotron Radiat*. 2006; 13:59. [PubMed: 16371709]
29. Minicozzi V, Stellato F, Comai M, Serra MD, Potrich C, Meyer-Klaucke W, Morante S. *J Biol Chem*. 2008; 283:10784. [PubMed: 18234670]
30. Hureau C. *Coord Chem Rev*. 2012; 256:2164.
31. Syme CD, Nadal RC, Rigby SEJ, Viles JH. *J Biol Chem*. 2004; 279:18169. [PubMed: 14978032]
32. Shearer J, Szalai VA. *J Am Chem Soc*. 2008; 130:17826. [PubMed: 19035781]
33. Cheignon C, Collin F, Faller P, Hureau C. *Dalton Trans*. 2016; 45:12627. [PubMed: 27264439]
34. Alies B, Badei B, Faller P, Hureau C. *Chem – Eur J*. 2012; 18:1161. [PubMed: 22189983]
35. Young TR, Kirchner A, Wedd AG, Xiao Z. *Metallomics*. 2014; 6:505. [PubMed: 24493126]
36. Feaga HA, Maduka RC, Foster MN, Szalai VA. *Inorg Chem*. 2011; 50:1614. [PubMed: 21280585]
37. Kau LS, Spira-Solomon DJ, Penner-Hahn JE, Hodgson KO, Solomon EI. *J Am Chem Soc*. 1987; 109:6433.
38. Himes RA, Park GY, Siluvai GS, Blackburn NJ, Karlin KD. *Angew Chem, Int Ed*. 2008; 47:9084.
39. Himes RA, Park GY, Barry AN, Blackburn NJ, Karlin KD. *J Am Chem Soc*. 2007; 129:5352. [PubMed: 17411054]
40. Alies B, Bijani C, Sayen S, Guillon E, Faller P, Hureau C. *Inorg Chem*. 2012; 51:12988. [PubMed: 23150940]

41. Hong L, Carducci TM, Bush WD, Dudzik CG, Millhauser GL, Simon JD. *J Phys Chem B*. 2010; 114:11261. [PubMed: 20690669]
42. Nakamura M, Shishido N, Nunomura A, Smith MA, Perry G, Hayashi Y, Nakayama K, Hayashi T. *Biochemistry*. 2007; 46:12737. [PubMed: 17929832]
43. Nadal RC, Rigby SEJ, Viles JH. *Biochemistry*. 2008; 47:11653. [PubMed: 18847222]
44. Noël S, Perez F, Pedersen JT, Alies B, Ladeira S, Sayen S, Guillon E, Gras E, Hureau C. *J Inorg Biochem*. 2012; 117:322. [PubMed: 22819647]
45. Alies B, Sasaki I, Proux O, Sayen S, Guillon E, Faller P, Hureau C. *Chem Commun*. 2013; 49:1214.
46. Strizhak P. *Theor Exp Chem*. 1994; 30:239.
47. Gottfredsen RH, Larsen UG, Enghild JJ, Petersen SV. *Redox Biol*. 2013; 1:24. [PubMed: 24024135]
48. Uehara H, Luo S, Aryal B, Levine RL, Rao VA. *Free Radical Biol Med*. 2016; 94:161. [PubMed: 26872685]

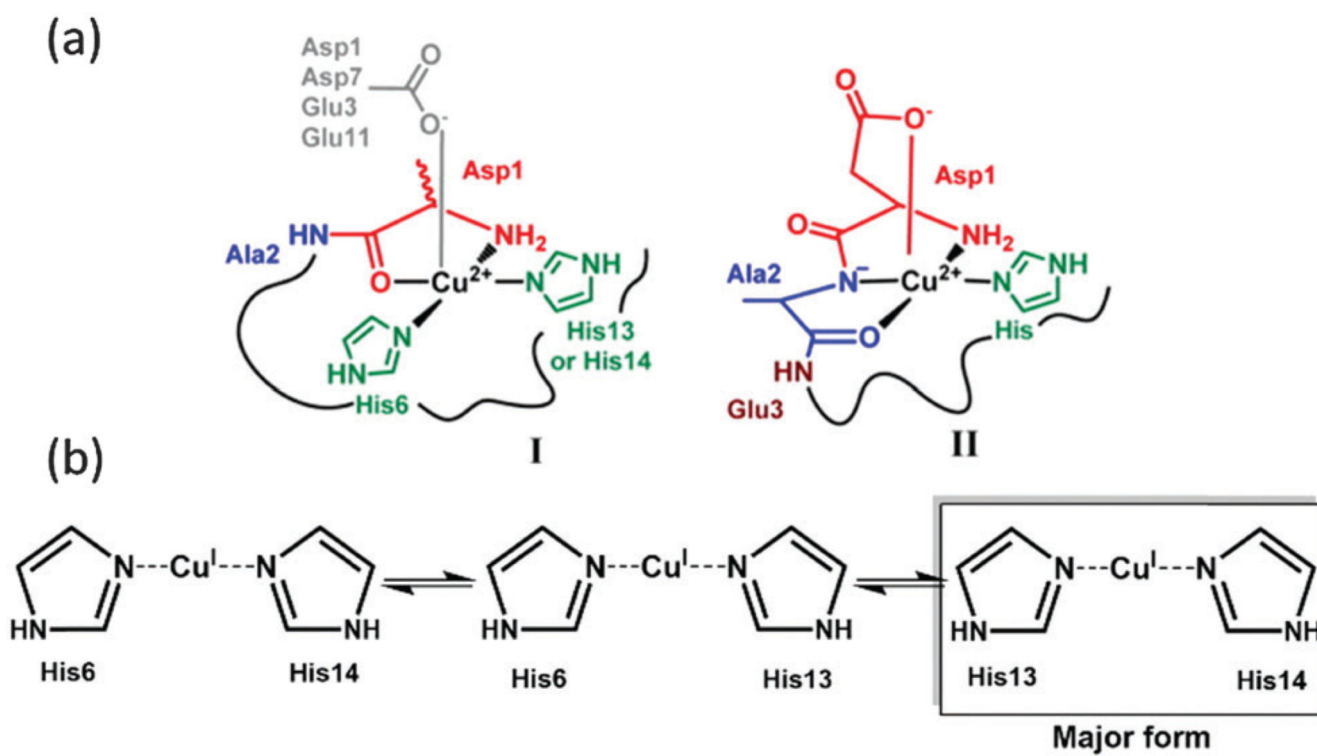


Fig. 1.

(a) Cu(II) coordination and (b) Cu(I) coordination to the A β peptide.^{16, 20}

DAEFRHDSGYEVHHQKLVFFAEDVGSNK

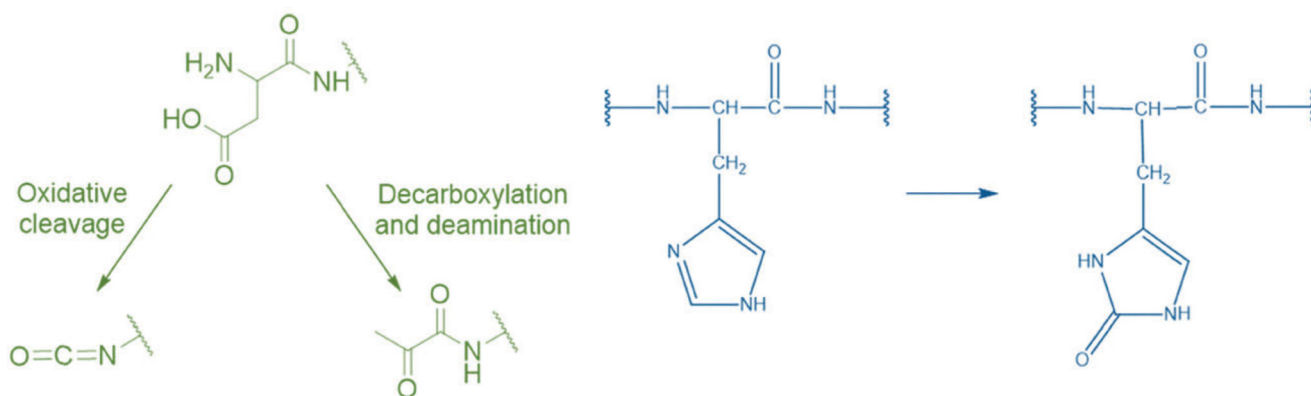


Fig. 2.

Amino acid sequence of the $\text{A}\beta_{28}$ peptide (top) along with the main targeted amino acid residues (in color) and the chemical structure of the oxidation products (bottom). Asp1 oxidation leads to the formation of either an isocyanate or a pyruvate function^{21,25} (green) and His13 and His14 oxidation reactions lead to the formation of 2-oxohistidines^{21,23,24} (blue).

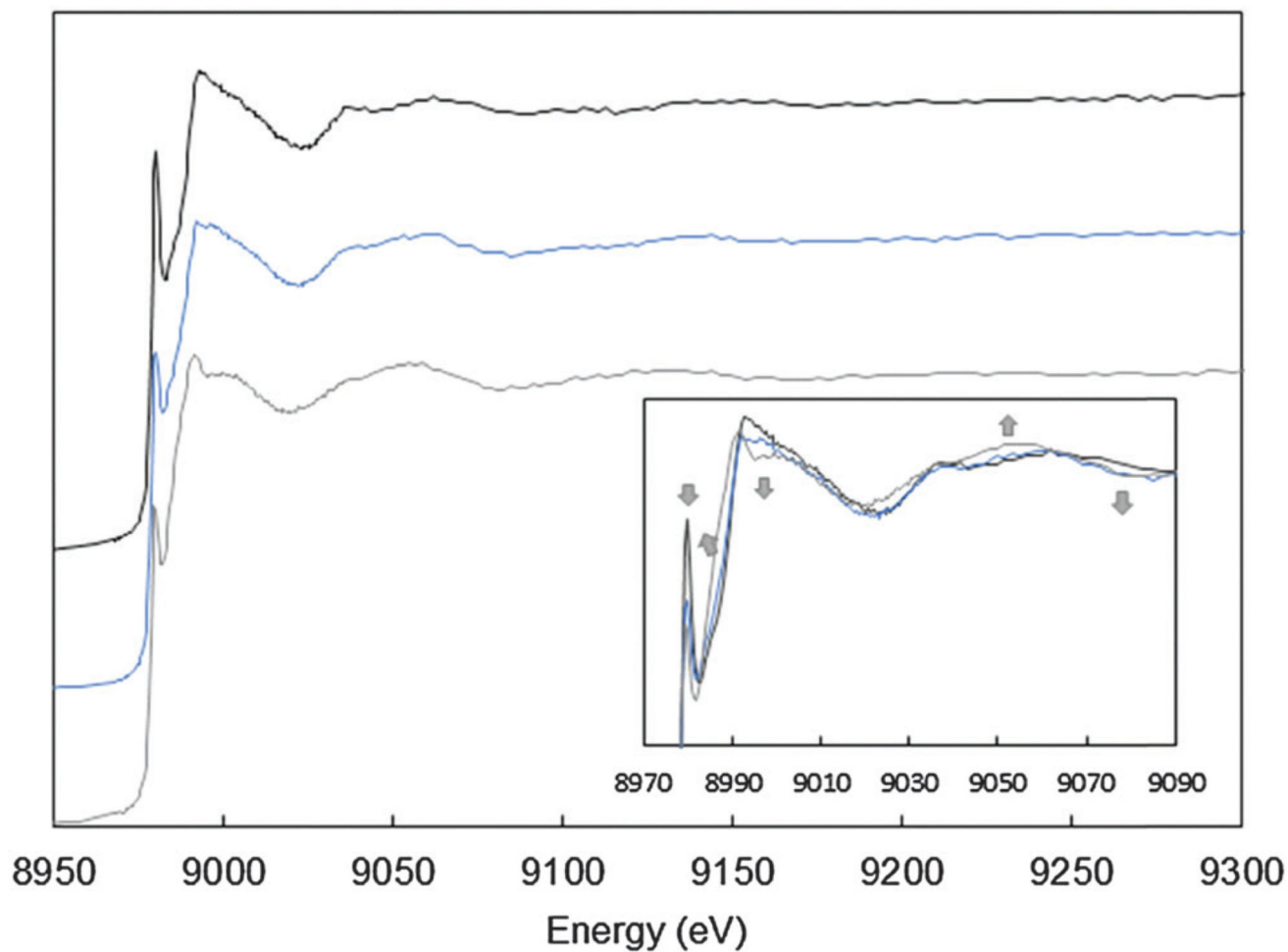


Fig. 3. Cu XANES K-edge X-ray absorption spectra of Aβ₂₈-Cu(I) (black curve), Aβ_{ox}-Cu(I) (blue curve) and Aβ₇-Cu(I) (grey curve). The conditions were as follows: 0.9 mM Cu(II), 1 mM peptide, and 10 mM dithionite in a HEPES buffer (0.1 M, pH 7.1) solution. Arrows indicate the evolution of the Aβ_{ox}-Cu(I) signature compared with the Aβ₂₈-Cu(I) signature. Inset: zoom of the 8970–9090 eV range.

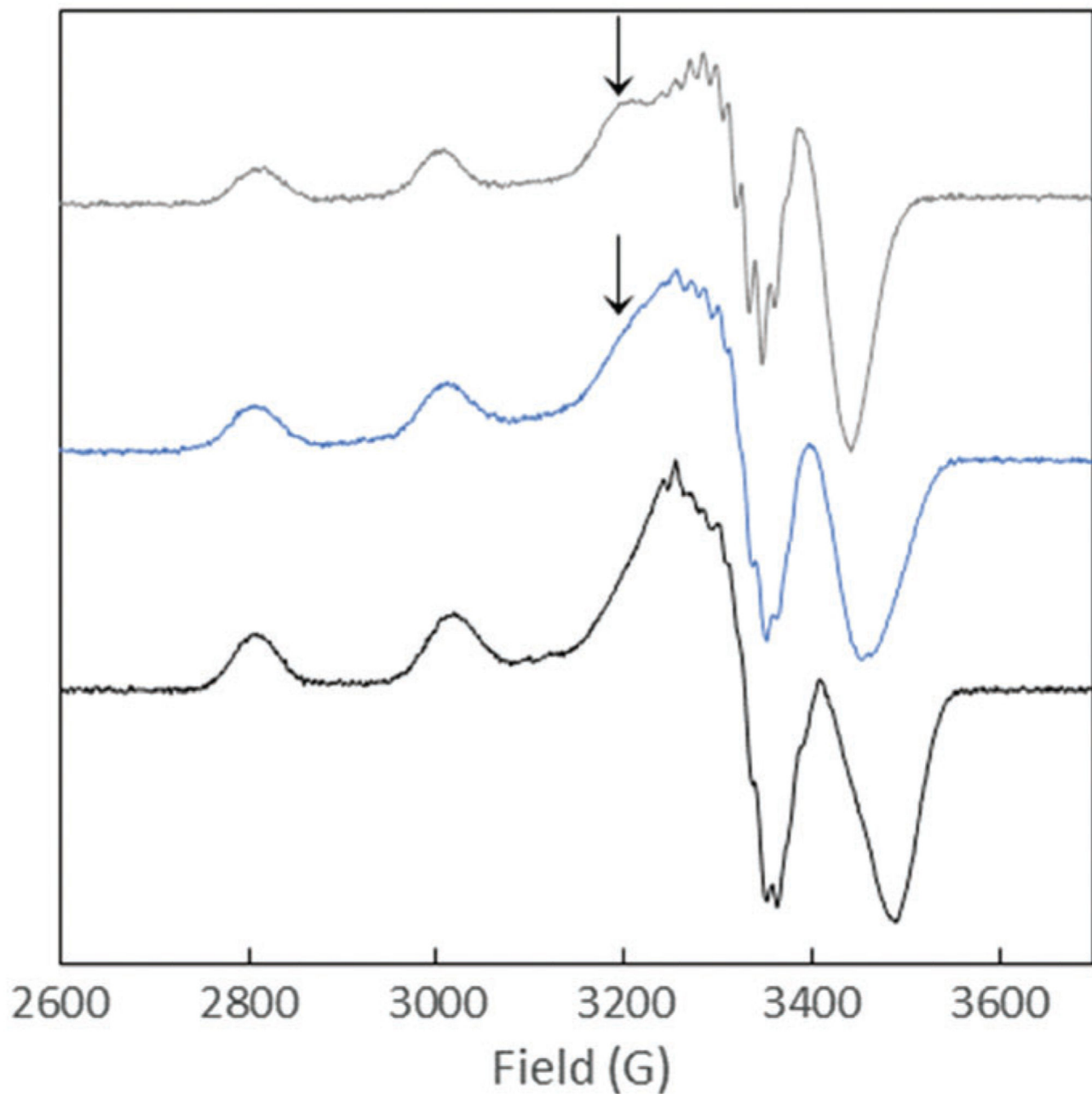


Fig. 4. EPR spectra of Cu(II)–A β ox (blue curve), Cu(II)–A β ₂₈ (black curve) and Cu(II)–AcA β ₂₈ (grey curve) at pH 12.5. Aqueous solution with 10% of glycerol containing ⁶⁵Cu (450 μ M) and peptide (500 μ M). $T = 120$ K, $\nu = 9.5$ GHz, microwave power = 20.5 mW, amplitude modulation = 10.0 G, and modulation frequency = 100 kHz.

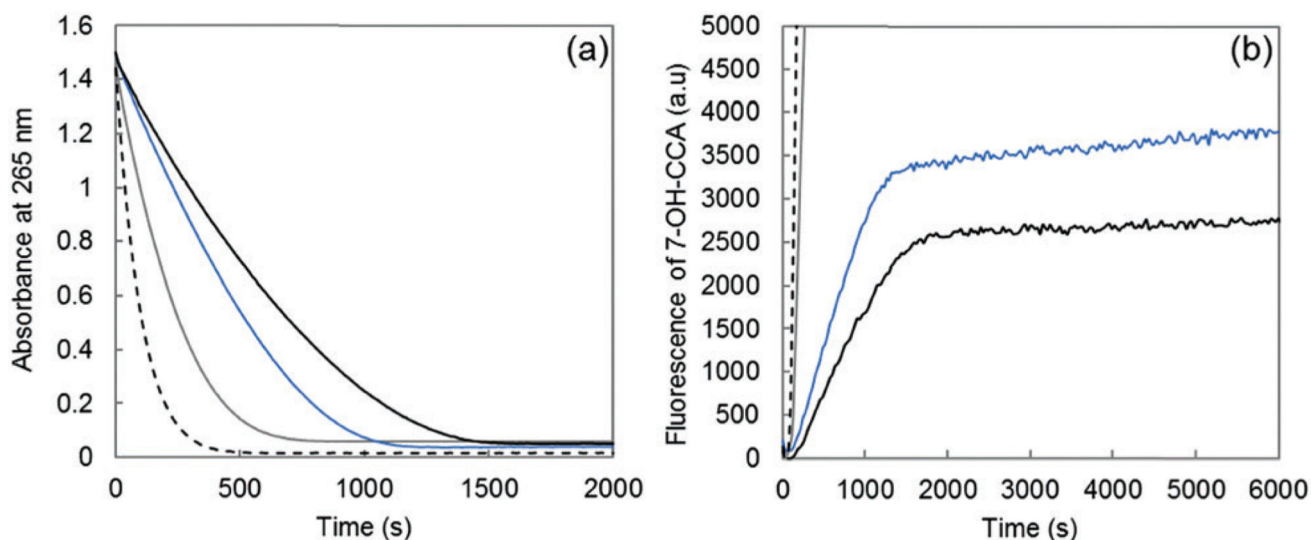
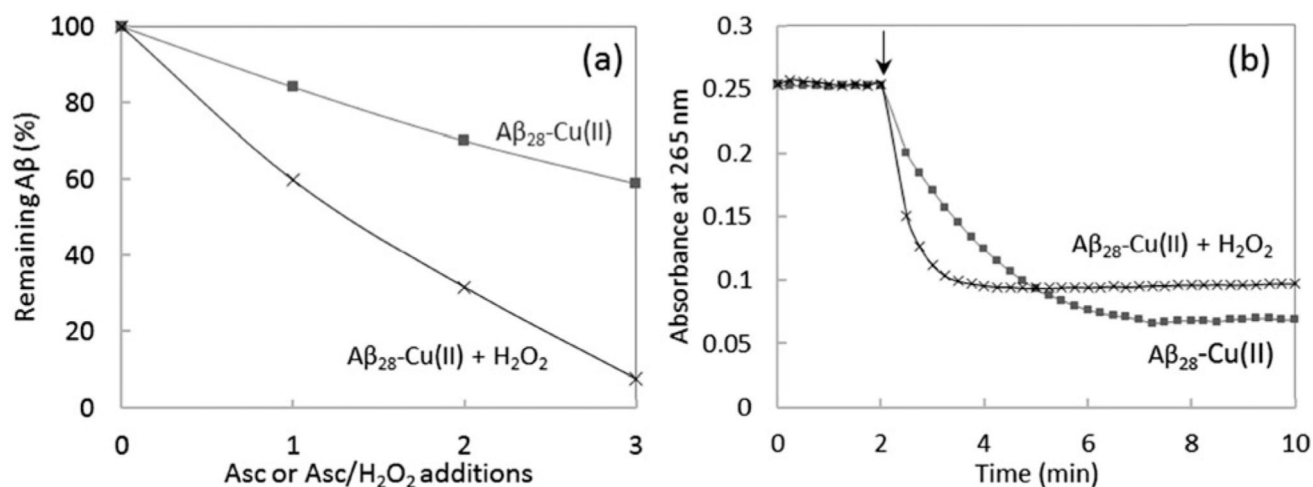


Fig. 5.

(a) Ascorbate consumption by Cu-Aβ₂₈ (black curve), Cu-Aβ_{ox} (blue curve), Cu-Aβ₇ (grey curve) and free Cu (dashed curve) measured using UV spectrophotometry ($\lambda = 265$ nm) as a function of the reaction time; phosphate buffered solution (50 mM, pH 7.4), Cu(II) 10 μ M, peptide 12 μ M and ascorbate 100 μ M. (b) Fluorescence as a function of the time of 7-OH-CCA resulting from the oxidation of CCA obtained for Cu-Aβ₂₈ (black curve), Cu-Aβ_{ox} (blue curve), Cu-Aβ₇ (grey curve) and free Cu (dashed curve); phosphate buffered solution (50 mM, pH 7.4), Cu(II) 50 μ M, peptide 60 μ M (oxidized or non-oxidized), ascorbate 500 μ M and CCA 500 μ M.

**Fig. 6.**

(a) Remaining non-oxidized Aβ₂₈ after successive additions of ascorbate (4 nmol, final conc. 20 μM) or ascorbate/H₂O₂ (4/10 nmol, final conc. 20/50 μM). Aβ₂₈ 25 μM and Cu²⁺ 20 μM, phosphate buffered pH 7.4 (50 mM). Ordinate: ratio between the peak area of non-oxidized Aβ₂₈ and the reference peak area of non-ox Aβ₂₈ (no addition of ascorbate nor H₂O₂). HPLC/HRMS, *m/z* 1087.8503, 816.1397, 653.1133 ([M + *n*H]^{*n*+}, *n* = 3, 4, 5), 5 ppm accuracy. (b) Ascorbate consumption measured at 265 nm as a function of the reaction time; Aβ₂₈ 25 μM, Cu²⁺ 20 μM, phosphate buffered pH 7.4 (50 mM), ascorbate 20 μM, with or without H₂O₂ 50 μM.

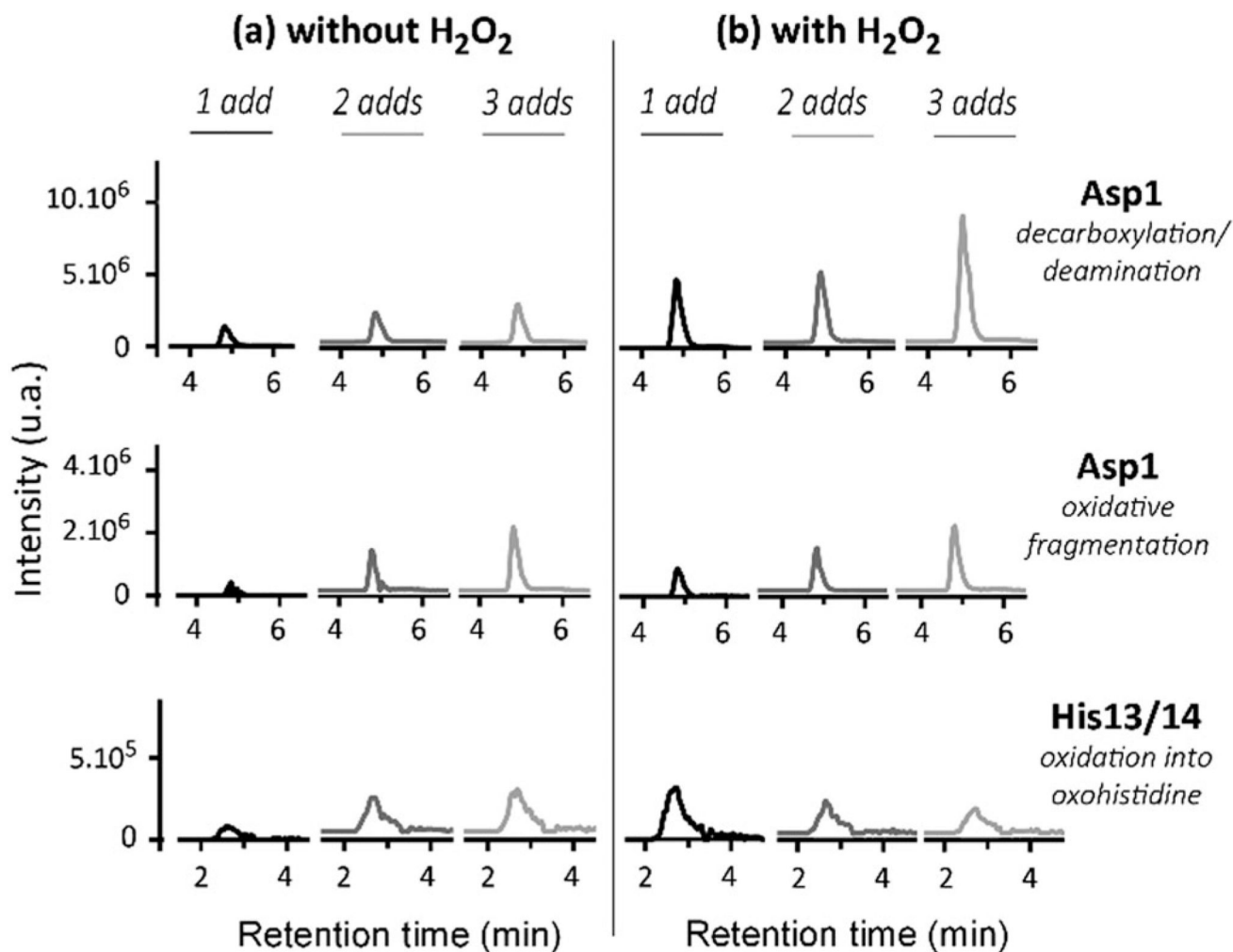


Fig. 7.

Oxidation of A β in the absence or presence of H₂O₂. Trace chromatograms obtained by HPLC/HRMS of the A β oxidized tryptic peptides DAEFR_{dd} (decarboxylation and deamination of Asp1), DAEFR_{ox} (oxidative fragmentation of Asp1), and HDSGYEVHHQK + 16 after 1 (black curve), 2 (dark grey curve) or 3 (light grey curve) additions of ascorbate (4 nmol, final conc. 20 μ M; left panel) or ascorbate/H₂O₂ (4/10 nmol, final conc. 20/50 μ M; right panel). A β ₂₈ 25 μ M and Cu(II) 20 μ M, phosphate buffered pH 7.4 (50 mM). Mass tolerance set at 5 ppm; *m/z* ratios used for the detection are specified in Table S1 (ESI⁺). The corresponding raw chromatograms are given in Fig. S7–S9 (ESI⁺). The oxidized residues were identified by HR-MS (Asp1 oxidation, see Table S2, ESI⁺) and by MS/MS (His13 and His14 oxidation reactions, see Fig. S10 and S11, ESI⁺).

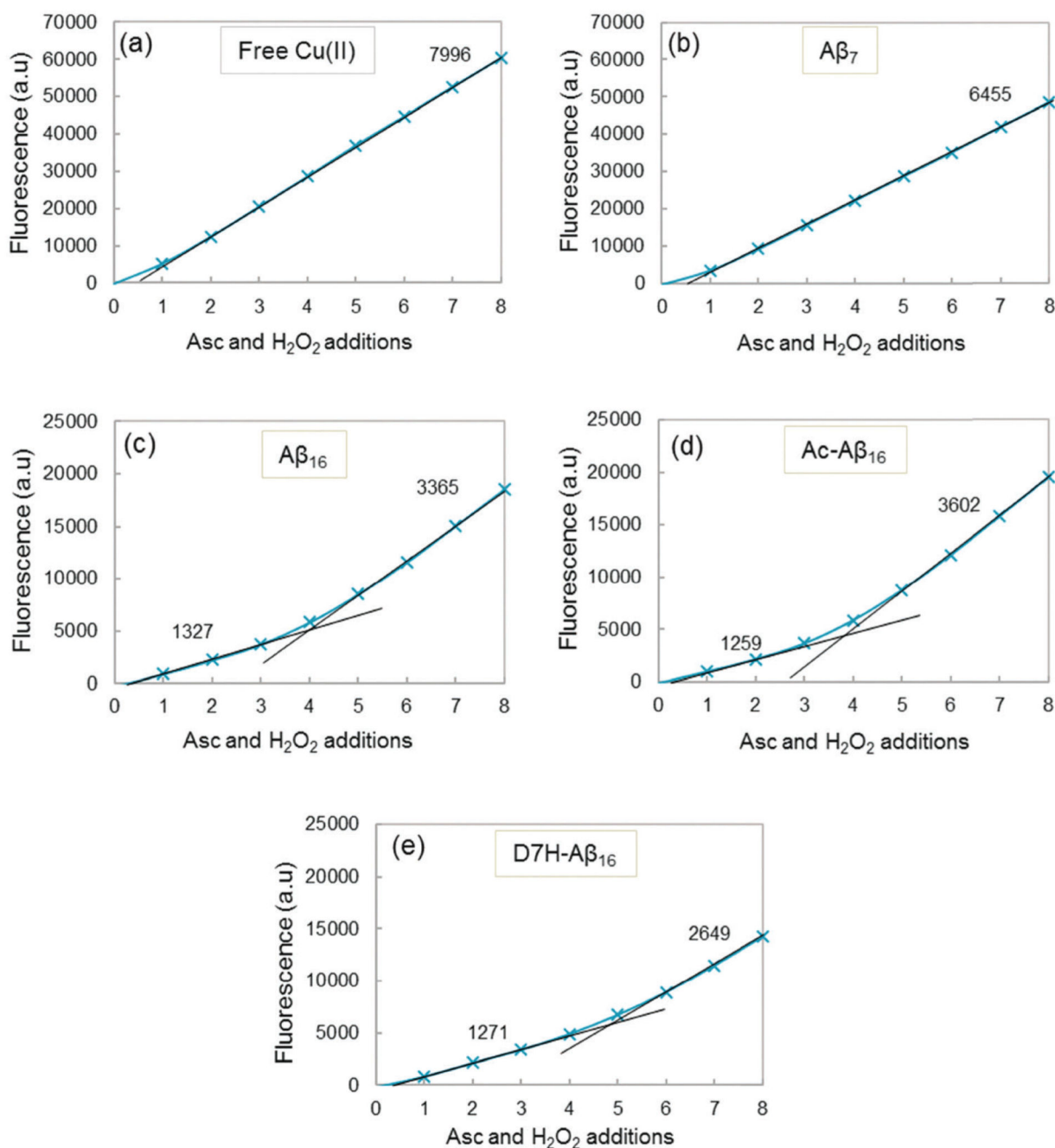


Fig. 8.

Cu–Aβ induced HO[•] trapped by CCA. Fluorescence intensity at the plateau of phosphate buffered solution (50 mM) containing Cu (20 μM), peptide (25 μM), and CCA (0.5 mM) as a function of the number of ascorbate and H₂O₂ additions. A total of 8 additions of 2 μL ascorbate (2 mM) and 2 μL hydrogen peroxide (5 mM) are realized, *i.e.* 4 and 10 nmol for each addition respectively (initial concentrations reaching 20 and 50 μM for the first addition, respectively). Gradients of the linear parts of the curves are indicated in black. The gradient and determination coefficients of fits for each curve are given in the ESI,† Table S3.

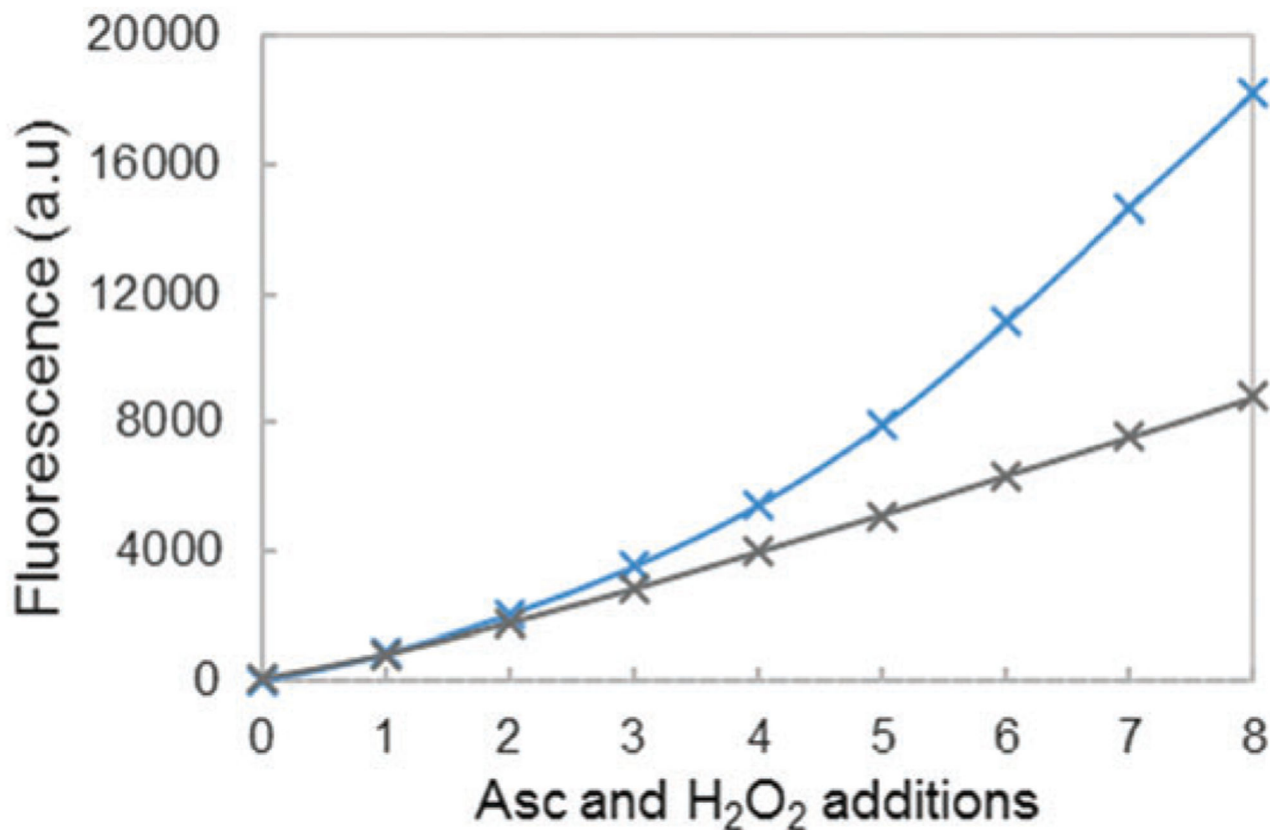
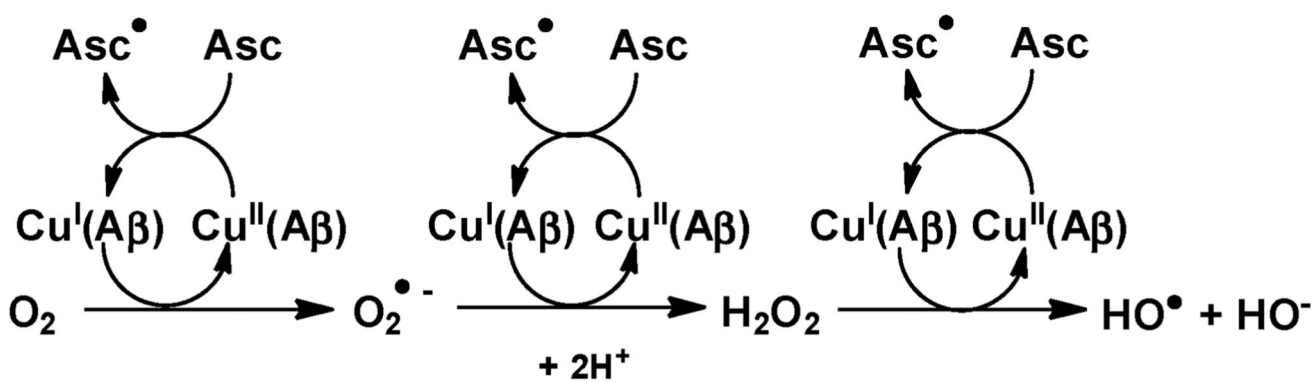


Fig. 9.

Fluorescence intensity at the plateau of phosphate buffered solution (50 mM) containing 20 μM of Cu, 25 μM (blue curve) or 50 μM (grey curve) of the A β_{16} peptide, and CCA (0.5 mM) as a function of the number of ascorbate and H₂O₂ additions. A total of 8 additions of 2 μL ascorbate (2 mM) and 2 μL hydrogen peroxide (5 mM) are realized, *i.e.* 4 and 10 nmol for each addition respectively (initial concentrations reaching 20 and 50 μM for the first addition, respectively). Gradients of the linear parts of the curves are indicated in black. The gradient and determination coefficients of fits for each curve are given in the ESI,† Table S3



Scheme 1.

Metal-catalyzed Reactive Oxygen Species (ROS) production in the presence of the amyloid- β peptide (A β); Asc = ascorbate, DHA = dehydroascorbate.